JOURNAL OF MOLECULAR SPECTROSCOPY 135, 289–304 (1989)

Microwave Spectrum, r_s Structure, and Internal Rotation of Methyl Fluorogermane

MICHIRO HAYASHI, SHOJI KAMINAKA, MASAHARU FUJITAKE,
AND SONOKO MIYAZAKI

*Department of Chemistry, Faculty of Science, Hiroshima University,
Higashi-sendamachi, Naka-ku, Hiroshima 730, Japan*

The microwave spectra of methyl fluorogermane and its 17 isotopic species were measured. The rotational, centrifugal distortion constants and the quantities related to the methyl internal rotation were simultaneously determined for the species having CH_3 and CD_3 groups. Quade-type analysis for the splittings of the spectra were carried out for CH_2DGeH_2F. From the observed moments of inertia, the r_s structure was well established. Discussions on the molecular structures were presented by comparing with the results of the analogous molecules. Especially, the angle relation of the GeH_2 group and the tilt angle of the methyl group were considered.

INTRODUCTION

The microwave spectra and molecular structure of methyl fluorogermane have been reported by Roberts *et al.* (*1*) and Krisher *et al.* (*2*). Roberts *et al.* concluded that the methyl group of this molecule tilts toward the fluorine atom by about 2° from the analysis of the *A–E* splittings of the spectra due to the methyl internal rotation.

Their paper called our attention since the direction of the tilt for methyl fluorogermane is opposite to the directions of the tilted methyl groups of molecules studied so far.

Then, one of the present authors had worked carefully on the microwave spectra and molecular structure of methyl fluorosilane which is considered to be an appropriate reference for methyl fluorogermane.

For methyl fluorosilane (*3*), it was noted that the directions of the methyl top axis obtained from the r_s structure and from the *A–E* splitting analysis do not coincide with each other. The direction of the tilt from the r_s structure inclines by 1°45′ from the direction of the CSi bond toward two hydrogen atoms attached to the silicon atom, while the direction obtained from the *A–E* splitting analysis inclines by 47′ toward the fluorine atom in a similar manner as the reported direction for methyl fluorogermane.

However, we could not conclude whether this fact has any physical meaning or not due to ambiguity in the r_s structure and the degree of approximation in the internal rotation analysis of the *A–E* splittings by the principal axis method.

The present investigation of the microwave spectra of methyl fluorogermane was carried out in order to reexamine the conclusions given by Roberts *et al.* and to compare the results with those of methyl fluorosilane when the procedures used for

0022-2852/89 $3.00

the analyses of the spectra of the present molecule were similar to those applied for methyl fluorosilane.

The measurements of the spectra were extended to the isotopically substituted species which were not measured by Roberts *et al.*

The A–E splittings of the observed spectra due to the methyl internal rotation were actually large; that is, some of the b-type transitions of the normal species are more than 30 MHz. Furthermore, for the a-CH_2DGeH_2F species, large splittings of the spectra were also found.

In order to determine the r_s structure, the rotational constants of all the isotopic species used should be obtained in the unperturbed state from the methyl and CH_2D type internal rotation.

For the CH_3 and CD_3 species, the A–E splittings of the spectra were easily predicted by the standard PAM-bootstrap analysis. On the other hand, the CH_2D type internal rotation splittings were predicted by the method proposed by Quade *et al.* (*4*).

The r_s structure was established and compared with that for methyl fluorosilane.

EXPERIMENTAL DETAILS

The samples of the normal and CH_3GeD_2F species used for the measurements were prepared from commercial methyl trichlorogermane by the following successive reactions: (i) methyl trichlorogermane was reduced by lithium aluminum hydride or deuteride in dibutyl ether, (ii) the resulting methyl germane or CH_3GeD_3 was reacted with bromine at liquid nitrogen temperature, and (iii) methyl bromogermane or CH_3GeD_2Br obtained was converted to methyl fluorogermane or CH_3GeD_2F by reacting with PbF_2 at room temperature.

The samples of $^{13}CH_3GeH_2F$, CD_3GeH_2F, and CH_2DGeH_2F, species were prepared from the appropriate isotopic species of methyl germane by the above reactions (ii) and (iii). The isotopic species of methyl germane were prepared from bromogermane or deuterated bromogermane and appropriate isotopic methyl Grignard reagent in dibutyl ether. Bromogermane or deuterated bromogermane was obtained by reducing tetrachlorogermane with sodium borohydride in water or with $LiAlD_4$ in dibutyl ether and germane obtained was reacted with bromine.

A conventional 100 kHz Stark modulation spectrometer was used for the measurements of the spectra at dry-ice temperature.

MICROWAVE SPECTRA

Methyl fluorogermane is a prolate asymmetric top molecule ($\kappa = -0.63$) with nonzero dipole moment components, μ_a and μ_b. Strong a-type transitions and weak b-type transitions are expected since μ_a is about 2.5 times larger than μ_b. Doublet structures are found for all the transitions of the isotopic species having the CH_3 group, while for isotopic species having the CD_3 group, a-type transitions are usually singlets and b-type transitions exhibit doublet structures. Singlets are found for the s-CH_2DGeH_2F species whose deuterium atom in the methyl group is situated in the molecular plane, while doublets are found for the a-CH_2DGeH_2F species whose deuterium atom is situated out of the molecular plane.

About 30 *a*- and *b*-type transitions with $J \leqslant 8$ and $K_a \leqslant 2$ were measured for all the species. The A–E splittings of some of the transitions were found to be more than 30 MHz.

The computer program used for the analysis was described in the previous paper (*5*) and could determine simultaneously the unperturbed rotational constants, quartic centrifugal distortion constants, and the quantities related to the methyl internal rotation from the observed frequencies for each of the CH_3 and CD_3 species.

For methyl fluorogermane, all the five quartic centrifugal distortion terms expressed in the Watson-A reduction (*6*) were found to be necessary to fit the observed frequencies. For the methyl internal rotation analysis, the standard PAM-bootstrap formula was used where the barrier V_3, the direction cosines of the methyl top axis and the moment of inertia of the methyl top around the top axis I_α were taken to be variables.

For the *s*-CH_2DGeH_2F and *a*-CH_2DGeH_2F species, the method proposed by Quade *et al.* was applied.

Observed frequencies are given in Tables I, II, and III.

ANALYSIS OF SPECTRA

For the isotopic species having CH_3 or CD_3 group, the first calculation was carried by regarding as variables all the parameters—rotational constants, five centrifugal distortion constants, barrier height V_3, one of direction cosines λ_a of the methyl top axis, and the top moment of inertia I_α.

As already reported in the previous paper on dimethyl silane and dimethyl sulfide (*5*), the top moment of inertia I_α is usually difficult to be determined from the A–E splitting analysis.

However, for methyl fluorogermane, I_α could be determined for the normal, CH_3GeD_2F, and $^{13}CH_3GeH_2F$ species. Though the error limits of the I_α values were large, the error limits were much smaller than the values determined for the other molecules. In order to reduce the influence of ambiguity of the I_α values, the I_α with the smallest error limit among the three Ge isotopic species was chosen for the normal, CH_3GeD_2F, and $^{13}CH_3GeH_2F$ species and the calculations were repeated as the I_α was fixed.

For CD_3GeH_2F species, reasonable I_α values could not be obtained and we used the value converted from that of the normal species. The results are listed in Table IVa.

The following procedures of the analysis were carried out for the isotopic species having CH_2D group. The spectra of the *s*-CH_2DGeH_2F species exhibit only singlets and they could be predicted well by the usual modified rigid rotor formula which contained five centrifugal distortion terms in the Watson-A reduction expression. Results are listed in Table IVb.

The spectra of the *a*-CH_2DGeH_2F species exhibit mainly doublets due to the tunnelling effect between two equivalent forms which produces the + and − states.

Since the observed transitions are *a*- and *b*-types, they are the transitions allowed under the selection rule $+\leftrightarrow+$ and $-\leftrightarrow-$. In order to obtain approximate unperturbed rotational constants of the *a*-CH_2DGeH_2F species, the averages of the corresponding

TABLE Ia

Observed Frequencies of Methyl Fluorogermane (MHz)[a]

Transition		CH$_3$GeH$_2$F			CH$_3$GeD$_2$F	
J'Ka'Kc' ← J"Ka"Kc'	^{74}Ge	^{72}Ge	^{70}Ge	^{74}Ge	^{72}Ge	^{70}Ge
$1_{01}-0_{00}$	10877.57(-1) 10876.36(15)	10886.96(3) 10885.65(9)	10896.77(1) 10895.38(-1)	10521.50(-5) 10520.47(13)	10529.36(-3) 10528.34(-16)	10537.47(-5) 10536.42(10)
$2_{02}-1_{01}$	21506.26(-11) 21503.85(8)	21530.14(-6) 21527.70(10)	21555.03(0) 21552.48(6)	20779.60(-9) 20777.40(4)	20799.95(-6) 20797.73(-4)	20821.04(-3) 20818.83(0)
$2_{12}-1_{11}$	20127.59(-8) 20129.43(3)	20155.79(-5) 20157.71(5)	20185.27(-2) 20187.17(5)	19547.24(-7) 19548.66(7)	19570.80(-6) 19572.22(9)	19595.30(-3) 19596.74(15)
$2_{11}-1_{10}$	23382.46(-10) 23375.95(11)	23391.84(-4) 23385.11(2)	23401.70(1) 23394.86(-1)	22538.65(-9) 22533.15(3)	22546.53(-3) 22540.88(-7)	22554.62(-5) 22548.91(-16)
$3_{03}-2_{02}$	31673.81(-8) 31670.35(6)	31720.68(-4) 31717.18(6)	31769.14(-5) 31765.66(8)	30560.91(-5) 30557.97(6)	30601.20(-4) 30598.04(2)	30642.58(-4) 30639.63(4)
$3_{13}-2_{12}$	30046.09(-4) 30045.15(16)	30091.26(-6) 30090.34(14)	30138.28(-5) 30137.37(17)	29168.44(0) 29167.56(16)	29206.30(-3) 29205.47(19)	29245.71(-3) 29244.82(12)
$3_{12}-2_{11}$	34904.01(-8) 34897.79(8)	34921.79(-5) 34915.67(23)	34940.46(-7) 34933.95(13)	33625.81(-1) 33620.38(9)	33640.98(-2) 33635.48(-1)	33656.72(-3) 33651.25(-1)
$3_{22}-2_{21}$	32632.81(-3) ——	32660.99(-7) ——	32690.46(2) ——	31654.56(-1) ——	31588.07(-4) ——	31612.56(-2) ——
$3_{21}-2_{20}$	33590.89(-9) ——	33600.51(-6) ——	33610.76(-9) ——	32657.54(-3) ——	32574.50(-3) ——	32581.96(-2) ——
$3_{12}-3_{13}$	9740.40(4) 9734.68(2)	9684.70(8) 9679.00(3)	9626.61(5) 9620.90(2)	8944.58(0) 8939.45(-3)	8898.31(3) 8893.17(-1)	8850.10(3) 8844.95(-3)
$4_{13}-4_{14}$	16107.08(6) 16095.68(7)	16018.57(5) 16007.14(-2)	15926.22(6) 15914.84(10)	14753.35(-1) 14743.25(-3)	14680.75(0) 14670.60(-9)	14605.03(6) 14595.88(-6)
$5_{14}-5_{15}$	23761.49(0) 23743.35(2)	23652.09(-1) 23623.94(-5)	32517.06(6) 23498.90(6)	21651.42(-1) 21635.45(-3)	21556.05(4) 21540.15(4)	21455.98(3) 21440.16(7)
$6_{15}-6_{16}$	32321.69(-2) 32295.70(-5)	32183.92(-3) 32158.00(-3)	32038.60(2) 32012.57(-4)	29210.33(2) 29187.61(-4)	29104.81(3) 29082.12(-9)	28993.14(1) 28970.48(-18)
$6_{24}-6_{25}$	12760.34(-1) 12758.15(-7)	12577.35(6) 12575.39(-5)	12387.76(3) 12385.73(-11)	12675.90(3) 12672.51(5)	12526.89(2) 12523.50(4)	12372.50(4) 12369.11(6)
$7_{25}-7_{26}$	19925.06(-8) 19916.75(-9)	19675.43(4) 19667.34(-4)	19415.80(3) 19407.67(-8)	19442.87(2) 19433.77(-6)	19245.25(-2) 19236.16(-9)	19039.78(2) 19030.70(-8)
$8_{26}-8_{27}$	28462.47(2) 28448.09(4)	28155.74(-4) 28140.69(-2)	27834.54(-9) 27819.61(13)	27299.09(-1) 27283.44(-12)	27064.41(-3) 27048.94(-2)	26819.05(-2) 26803.58(-8)
$2_{11}-2_{02}$	10618.32(12) 10608.17(0)	10672.99(5) 10662.68(-9)	10730.61(5) 10720.30(-7)	8815.41(2) 8807.95(7)	8846.56(6) 8839.07(8)	8879.45(5) 8871.87(-3)
$3_{12}-3_{03}$	13848.51(12) 13835.40(-18)	13874.16(11) 13861.02(-8)	13091.69(7) ——	11880.29(4) 11870.27(1)	11996.50(6) 11876.49(3)	11893.60(7) 11882.50(-6)
$4_{13}-4_{04}$	18728.05(11) 18711.45(-11)	18709.53(6) 18692.93(-3)	18691.26(7) 18674.52(-9)	16501.52(3) 16488.25(5)	16471.73(6) 16348.28(-11)	16441.33(7) 16427.84(-16)
$5_{14}-5_{05}$	25277.67(12) 25256.17(-6)	25210.40(4) 25188.80(-16)	25141.00(8) 25119.29(-14)	22589.33(4) 22571.45(-1)	22523.63(9) 22505.67(-7)	22455.23(6) 22437.35(-6)
$6_{15}-6_{06}$	33136.70(5) 33108.84(-13)	33033.48(4) 33005.84(15)	32925.30(4) 32897.17(-17)	29677.61(3) 29653.88(-8)	29590.26(4) 29566.67(-10)	29398.15(3) —— (3)
$3_{22}-3_{13}$	28811.58(-4) 28756.06(4)	29002.15(-2) 28945.12(-3)	29202.41(-10) 29145.00(1)	23564.55(1) ——	23681.15(4) ——	23803.37(8) ——
$4_{23}-4_{14}$	32305.36(-6) 32262.33(14)	32473.04(-8) 32429.20(13)	32649.68(1) 32605.50(12)	26799.37(1) 26766.93(9)	26896.79(1) 26864.45(19)	26999.04(7) 26966.70(23)
$3_{21}-3_{12}$	20277.99(-13) 20273.87(26)	20500.50(07) 20496.75(24)	20734.64(-4) 20731.02(2)	15886.19(-1) 15882.32(7)	16027.85(1) 16024.00(-5)	16176.50(5) 16172.61(-21)
$4_{22}-4_{13}$	19603.23(-6) 19585.94(-18)	19797.53(-5) 19790.10(-10)	20002.89(0) 19985.56(0)	15562.23(-3) 15549.51(-11)	15678.67(3) 15665.90(-14)	15801.44(6) 15799.65(-18)
$5_{23}-5_{14}$	20147.97(1) 20128.15(4)	20290.21(-1) 20270.10(-4)	20442.07(0) 20421.93(0)	16503.80(-3) 16489.37(3)	16575.72(-3) 16561.18(-8)	16652.73(0) 16638.20(-4)
$6_{24}-6_{15}$	22339.79(1) 22319.21(3)	22405.86(2) 22384.84(-9)	22479.23(0) 22458.10(-8)	19081.69(-2) 19066.00(-14)	19090.18(-5) 19074.57(-5)	19101.76(1) 19085.91(-21)
$7_{25}-7_{16}$	26460.62(-9) 26438.62(18)	26429.62(2) 26407.40(5)	26402.40(-1) 26370.02(-6)	23495.75(-2) 23479.15(-5)	23427.65(1) 23410.06(1)	23359.47(-1) 23341.85(-1)
$8_{26}-8_{17}$	32573.56(-9) 32548.85(18)	32438.27(-6) 32413.38(13)	32301.83(-2) 32276.73(2)	29634.92(-4) 29635.12(28)	29504.86(-4) 29483.99(20)	29359.63(-6) 29338.86(27)
$2_{12}-1_{01}$	27242.15(-1) 27229.98(-2)	27348.96(-7) 27336.60(-5)	27461.00(6) 27448.38(-15)	25107.84(-3) 25098.80(7)	25182.89(-1) 25173.83(6)	25261.42(2) 25252.36(6)
$3_{13}-2_{02}$				33496.62(-1) 33488.49(-20)	33589.22(1) 33581.15(-14)	33686.13(5) 33678.70(-10)
$3_{03}-2_{12}$	25937.96(-14) 25944.26(20)	25901.83(-6) 25908.00(-7)	25863.15(-12) 25869.44(-3)	26232.72(-6) 26236.70(9)	26218.10(-7) 26222.20(19)	26202.18(-11) 26206.28(16)

a. Figures in parentheses indicate the difference between the observed and calculated frequencies. The bar indicates the component of the doublet could not be measured due to some reasons. For example, the line was overlapped by the other strong line and so on. The transition with only one entry means unresolved doublet.

TABLE Ib

Observed Frequencies of Methyl Fluorogermane (MHz)[a]

Transition		$^{13}CH_3GeH_2F$			CD_3GeH_2F	
J'Ka'Kc' ← J"Ka"JKc"	^{74}Ge	^{72}Ge	^{70}Ge	^{74}Ge	^{72}Ge	^{70}Ge
$1_{01} - 0_{00}$	10557.01(-5) 10555.98(11)	10566.31(-6) 10565.30(12)	10575.90(-8) 10574.91(12)	9443.06(2)	9342.23(1)	9361.68(0)
$2_{02} - 1_{01}$	20883.56(-7) 20881.30(-3)	20906.97(-6) 20904.78(5)	20931.14(-7) 20928.95(4)	18705.54(0)	18727.64(0)	18750.54(5)
$2_{12} - 1_{11}$	19550.87(-5) 19553.15(8)	19578.73(-7) 19580.99(2)	19607.63(-7) 19609.94(0)	17577.29(-1)	17603.56(-2)	17630.92(1)
$2_{11} - 1_{10}$	22677.19(-7) 22670.89(10)	22686.48(-8) 22680.16(10)	22696.02(-13) 22689.80(20)	20194.85(6)	20205.22(4)	20215.88(6)
$3_{03} - 2_{02}$	30780.60(-6) 30777.43(5)	30826.10(-9) 30823.03(12)	30873.23(-9) 30870.20(16)	27628.65(2)	27670.13(0)	27713.21(5)
$3_{13} - 2_{12}$	29291.34(-7) 29190.66(11)	29235.75(-7) 29235.13(16)	29281.97(-5) 29281.31(12)	26249.78(3)	26201.25(-3)	26344.60(2)
$3_{12} - 2_{11}$	33859.06(-6) 33853.57(16)	33876.38(-8) 33870.94(20)	33894.38(-9) 33888.94(20)	20170.20(9)	30188.38(6)	30207.29(9)
$3_{22} - 2_{21}$	31671.29(-2) ——	31699.07(7) ——	32178.00(-6) ——	28329.20(-12)	28356.64(-10)	28385.32(-3)
$3_{21} - 2_{20}$	32561.14(-5) ——	32571.18(-8) ——	32581.97(-4) ——	29029.14(-5) ——	29042.55(7) ——	29056.77(-7) ——
$3_{12} - 3_{13}$	9357.23(-5) 9352.70(2)	9302.33(-1) ——	9245.22(4) 9240.75(14)			
$4_{13} - 4_{14}$	15481.93(-3) ——	15394.44(0) ——	15303.18(-3) ——	12978.30(-4) ——	12902.60(1) 12901.85(-3)	12823.20(-1) 12822.40(-9)
$5_{14} - 5_{15}$	22865.07(6) ——	22746.15(3) ——	22621.65(0) ——	19204.10(2) ——	19099.40(9) ——	18989.57(5) ——
$6_{15} - 6_{16}$				26252.40(5) ——		
$6_{24} - 6_{25}$	12000.26(-6) ——	11821.83(-4) ——	11637.20(2) ——	9650.80(-8)	9503.23(-5)	9349.90(-8)
$7_{25} - 7_{26}$	18821.90(4) ——	18576.62(1) ——	18321.72(-2) ——	15260.69(1)	15054.30(-9)	14839.43(-8)
$8_{26} - 8_{27}$				22061.35(-4) 22060.95(10)	21799.64(2) 21799.18(8)	21526.62(-3) 21526.21(11)
$2_{11} - 2_{02}$	10474.74(-2) 10464.76(5)	10530.99(1) 10520.90(1)	10590.03(-6) 10579.87(-2)			
$3_{12} - 3_{03}$	13553.18(-4) 13540.64(-9)	13851.25(-1) 13568.59(-13)	13611.25(1) 13598.62(3)	11761.52(0) 11760.39(-3)	11787.24(2) 11786.10(-2)	11814.50(2) 11813.46(8)
$4_{13} - 4_{04}$	18202.71(-3) 18187.38(6)	18187.58(1) 18172.17(9)	18172.75(2) 18157.00(-15)	15596.74(-1) 15595.50(-1)	15586.13(-1) 15584.90(0)	15575.72(3) 15574.49(3)
$5_{14} - 5_{05}$	24467.57(8) 24447.96(0)	24403.54(3) 24383.83(-9)	24337.47(4) 24317.71(-6)	20796.39(3) 20794.90(-1)	20742.66(-3) 20741.20(-4)	20687.39(6) 20685.91(3)
$6_{15} - 6_{06}$	32036.65(5) 32011.30(-13)	31934.75(10) 31909.36(-9)	31827.87(11) 31802.46(-7)	27153.45(8) 27151.46(-12)	27062.69(6) 27060.70(-15)	26968.40(12) 26966.30(20)
$3_{22} - 3_{13}$	28521.56(1) ——	28715.61(-1) ——	28919.72(-6) ——	25260.74(-2) 25257.94(10)	25428.49(-4) 25425.64(3)	25604.65(-5) 25601.86(6)
$4_{23} - 4_{14}$	31871.24(6) ——	32042.90(0) ——	32223.72(0) ——	28056.08(1) 28053.05(-3)	28204.76(7) 28201.82(12)	28361.06(1) 28358.03(-6)
$3_{21} - 3_{12}$	20284.50(4) 20281.06(-20)	20510.90(-2) ——		18304.20(-1) 18301.75(-11)	18501.38(-1) 18498.92(-11)	—— ——
$4_{22} - 4_{13}$	19561.40(7) 19543.87(12)	19761.19(-1) 19743.62(0)	19972.30(-3) 19954.71(8)	17586.07(-2) 17583.80(-9)	17763.09(0) 17750.82(-6)	17949.88(0) 17947.68(-1)
$5_{23} - 5_{14}$	18870.22(8) 19949.72(-16)	20120.20(-1) 20099.79(-3)	20280.22(2) 20259.53(-1)	17754.48(2) 17752.56(10)	17892.08(-3) 17890.10(1)	18038.47(0) 18036.46(-1)
$6_{24} - 6_{15}$	21926.80(6) 21906.12(-6)	22003.38(-1) 21982.73(10)	22087.70(2) 22066.64(-1)	19164.90(0) 19163.25(16)	18243.32(1) 19241.52(3)	19328.60(0) 19436.90(12)
$7_{25} - 7_{16}$				22067.05(-3) 22065.42(-1)		22072.05(-3) 22070.38(-3)
$8_{26} - 8_{17}$				26579.71(-1) 26578.08(-6)	26490.24(-4) 26488.71(1)	26401.50(-4) 26399.97(3)
$2_{12} - 1_{01}$				23999.19(-4) 23998.25(-2)	24094.10(-6) 24093.23(3)	24193.34(-9) 24192.45(-3)
$3_{13} - 2_{02}$				31553.41(-1) 31552.59(9)	31667.75(-2) 31666.90(4)	31787.45(-5) 31786.60(1)
$3_{03} - 2_{12}$	24995.42(-5) ——	24956.82(-8) ——	24915.80(-15) ——	22335.04(-11) 22336.76(5)	22303.71(-11) ——	

---

a. See the footnote of Table I-a.

TABLE II

Observed Frequencies of *s*-CH_2DGeH_2F Species (MHz)[a]

Transition J'Ka'Kc' ← J"Ka"Kc"	^{74}Ge	^{72}Ge	^{70}Ge
$1_{01}-0_{00}$	10188.90(0)	10197.34(-1)	10206.30(1)
$2_{02}-1_{01}$	20192.26(0)	20213.00(-2)	20234.75(0)
$2_{12}-1_{11}$	18946.16(0)	18971.63(2)	18998.31(1)
$2_{11}-1_{10}$	21809.40(0)	21817.82(-1)	21826.82(0)
$3_{03}-2_{02}$	29844.35(0)	29884.20(-1)	29925.47(1)
$3_{13}-2_{12}$	28309.76(0)	28350.23(0)	28392.33(-1)
$3_{12}-2_{11}$	32589.21(-1)	32604.61(1)	32620.80(0)
$3_{12}-3_{13}$	8574.33(-3)	8523.80(-5)	8471.30(1)
$4_{13}-4_{14}$	14210.16(-2)	14128.79(3)	14043.95(-1)
$5_{14}-5_{15}$	21059.50(-1)	20946.04(0)	20827.55(0)
$6_{15}-6_{16}$		28724.97(0)	28579.29(0)
$6_{24}-6_{25}$	10148.70(1)	9992.44(1)	9830.87(0)
$7_{25}-7_{26}$	16167.92(1)	15946.88(0)	15717.54(-1)
$8_{26}-8_{27}$	23536.58(0)	23252.95(0)	22957.60(1)
$2_{11}-2_{02}$	10578.26(-1)	10636.36(1)	10697.40(1)
$3_{12}-3_{03}$	13323.13(-1)	13356.83(-1)	13392.72(-1)
$4_{13}-4_{04}$	17459.14(2)	17454. (2)	17450.46(2)
$5_{14}-5_{05}$	23092.67(1)	23040.89(-1)	22097.95(-1)
$6_{15}-6_{06}$	30049.08(0)	29954.60(0)	29856.43(0)
$3_{22}-3_{13}$	29139.12(1)	29335.43(1)	29541.53(-1)
$4_{23}-4_{14}$	32187.54(2)	32363.50(-1)	32548.62(2)
$3_{21}-3_{12}$	21471.88(-2)	21700.60(-1)	21940.77(1)
$4_{22}-4_{13}$	20575.80(0)	20794.35(1)	21004.08(-3)
$5_{23}-5_{14}$	20586.02(-1)	20754.05(0)	20932.38(-1)
$6_{24}-6_{15}$	21897.84(1)	22004.12(0)	22118.90(0)
$7_{25}-7_{16}$			24849.14(1)
$8_{26}-8_{17}$	29441.85(-1)	29368.03(0)	29296.30(0)
$2_{12}-2_{01}$	26475.64(1)	26580.00(0)	26689.30(1)
$3_{03}-3_{12}$	23560.99(1)	23517.24(1)	23470.90(0)

a. Figures in parentheses indicate the difference between the observed and calculated frequencies.

frequencies for the transitions of the + and − states were taken and fitted by the usual modified rigid rotor formula. It was found that the average frequencies of the transitions could be predicted though the RMS value (the root-mean square deviation between the observed and calculated frequencies) was slightly larger than that for the *s*-CH_2DGeH_2F species.

The first determination of the r_s structure was made using the rotational constants determined for the species having the CH_3 or CD_3 group and the approximate rotational constants for the CH_2DGeH_2F species. The pure torsional energy levels of the CH_2DGeH_2F species were computed from the r_s coordinates and the V_3 obtained for the normal species by the formulation proposed by Quade *et al.* and the effective rotational Hamiltonian was derived up to the fourth order by perturbation formulae.

TABLE III

Observed Frequencies of the *a*-CH_2DGeH_2F Species (MHz)[a]

Transition	a-$CH_2D^{74}GeH_2F$		a-$CH_2D^{72}GeH_2F$		a-$CH_2D^{70}GeH_2F$	
$J'_{Ka'Kc'} \leftarrow J''_{Ka''Kc''}$	+state	-state	+state	-state	+state	-state
$1_{01} - 0_{00}$	10432.82(1)		10422.07(-4)		10451.98(-1)	
$2_{02} - 1_{01}$	20618.34(-1)		20642.21(0)		20667.25(7)	
$2_{12} - 1_{11}$	19308.56(1)		19336.60(2)		19365.84(-7)	
$2_{11} - 1_{10}$	22422.76(3)	22422.24(-3)	22432.16(6)	22431.55(-3)	22442.31(12)	22441.50(-12)
$2_{12} - 1_{01}$	25829.47(-2)	25828.21(1)			26038.36(2)	26036.85(-2)
$2_{11} - 2_{02}$	9882.60(0)	9880.62(1)	9932.81(2)	9930.80(-1)	9985.78(1)	9983.67(1)
$3_{03} - 2_{02}$	30348.36(-2)	30347.77(2)	30395.47(1)	30394.88(6)	30444.10(-1)	30443.43(2)
$3_{13} - 2_{12}$	28818.66(-1)	——	——	28863.40(-2)	28910.60(2)	——
$3_{12} - 2_{11}$	33464.95(3)	33464.74(0)	33483.05(1)	33481.76(-4)	33501.81(3)	33500.46(-2)
$3_{03} - 2_{12}$	——	25137.80(-2)	25106.42(-2)	——	25073.10(-1)	——
$3_{12} - 3_{13}$	9317.83(5)	9316.10(2)	9263.04(-3)	9261.17(-3)	9205.96(3)	9204.15(-2)
$3_{12} - 3_{03}$	——	12996.60(0)	13020.40(3)	13017.78(0)	13043.37(-4)	13040.71(-1)
$3_{22} - 3_{13}$	26713.32(5)	26707.62(-1)	26890.05(-10)	26884.49(6)	27076.29(-8)	27071.00(1)
$4_{13} - 4_{14}$	15398.70(-3)	15395.83(-5)	15312.18(8)	15309.11(5)		
$4_{13} - 4_{04}$	17706.64(5)	17703.20(0)	17684.36(-3)	17680.87(-2)	17662.31(4)	17658.77(4)
$4_{23} - 4_{14}$	30062.81(-10)	30056.70(1)	30217.50(6)	30211.24(-2)	30380.11(3)	30374.22(5)
$4_{22} - 4_{13}$	18027.00(2)	18023.08(-4)	18206.45(8)	18202.53(-6)	18395.60(0)	18391.90(-9)
$5_{14} - 5_{15}$	22687.85(0)	22683.67(8)	22571.87(3)	22567.41(-2)		
$5_{14} - 5_{05}$	23997.26(1)	23992.62(-6)	23928.31(-6)	23923.70(1)	23857.09(-2)	23852.41(-4)
$5_{23} - 5_{14}$	18669.15(2)	18665.30(2)	18796.22(-3)	18792.42(1)	18932.10(13)	18928.29(3)
$6_{24} - 6_{25}$	12475.39(0)	12473.43(2)			12108.11(0)	12105.95(3)
$6_{24} - 6_{15}$	20922.33(4)	20918.20(1)	20973.62(-3)	20969.45(-3)	21031.37(-1)	21027.26(-3)
$7_{25} - 7_{26}$	19288.48(-6)	19285.29(-5)	19144.34(-3)	19140.95(-2)	18890.38(-1)	18886.98(-3)
$7_{25} - 7_{16}$	25043.12(-3)	25038.50(4)	24999.18(6)	24994.40(-5)	24957.96(-8)	24953.29(2)
$8_{26} - 8_{17}$	31054.38(-1)	31048.66(-4)	30910.70(-5)	30905.10(0)	30765.12(1)	30759.42(2)
$8_{26} - 8_{27}$	27572.52(5)	27567.78(4)	27274.56(4)	27269.80(0)	26963.22(3)	26958.45(-1)

a. Figures in parentheses indicate the difference between the observed and calculated frequencies. The bar indicates the component could not be measured by some reasons. The transition with only one entry means an unresolved line.

For the $CH_2D^{74}GeH_2F$ species, pure torsional energy levels E^v_σ are found to array in the increasing energy order of E^0_+, E^0_-, E^0_s, E^1_-, E^1_+, E^1_s . . . , where σ stands for the + and − states of the *a*-CH_2DGeH_2F and the *s*-CH_2DGeH_2F species and v stands for the torsional quantum numbers.

For CH_2DCHO molecule, this ordering is reported by Turner *et al.* (*7*) to be E^0_s, E^0_+, E^0_- . . . and our calculation using the same computer program as that used for the CH_2DGeH_2F molecule gives the same ordering of the energy levels.

The energy differences $\Delta E(\sigma, \sigma') = E^0_\sigma - E^0_{\sigma'}$, between the levels are computed to be $\Delta E^0(-, +) = 160$, $\Delta E^0(s, -) = 59\,670$ MHz, respectively, where the V_3 is assumed to be 950 cal/mol and $\Delta E^0\ (-, +) = 215$, $\Delta E^0(s, -) = 57\,800$ MHz when the assumed V_3 is 900 cal/mol.

Furthermore, it is found that the mixing between E^0_s and E^0_+ states is very slight and the mixing between E^0_s and E^0_- is forbidden from the symmetry so that the rotational constants of the *s*-CH_2DGeH_2F species determined above can be safely regarded to be the unperturbed rotational constants of this species.

The derived effective rotational Hamiltonian for the CH_2DGeH_2F species indicates that the effective rotational constants of the + and − states of the *a*-CH_2DGeH_2F species show very small differences with each other and the terms connecting these two states are also so small that they are negligible unless the rotational energy levels are in near degeneracy between the + and − states.

In order to find the possibility of near degeneracy, the spectra for the + and − states were fitted in the usual modified rigid rotor formula, separately, and the approximate rotational constants for the + and − states were obtained. The differences of the

TABLE IVa

Rotational, Centrifugal Distortion Constants,[a] and Quantities Related to the Methyl Internal Rotation of Methyl Fluorogermane

		CH_3GeH_2F			CH_3GeD_2F	
	^{74}Ge	^{72}Ge	^{70}Ge	^{74}Ge	^{72}Ge	^{70}Ge
A (MHz)	13359.964(101)	13438.511(84)	13520.962(83)	11563.920(72)	11615.390(76)	11669.442(91)
B (MHz)	6251.735(39)	6251.696(33)	6251.695(31)	6007.954(29)	6007.942(31)	6007.909(37)
C (MHz)	4625.027(38)	4634.415(32)	4544.246(30)	4512.886(28)	4520.739(30)	4528.900(36)
Δ_J (kHz)	7.18(242)	5.80(202)	6.99(193)	6.95(175)	6.95(186)	5.52(224)
Δ_{JK} (kHz)	-37.38(175)	-38.95(146)	-38.63(134)	-27.99(154)	-28.57(163)	-26.12(196)
Δ_K (kHz)	111.38(2182)	134.70(1823)	130.20(1791)	66.06(1571)	60.18(1673)	93.11(2003)
δ_J (kHz)	2.56(8)	2.53(7)	-2.56(6)	2.24(6)	2.26(6)	2.34(8)
δ_K (kHz)	1.45(130)	2.45(110)	0.04(3)	0.34(89)	-0.14(96)	-3.50(123)
I_α (amu·Å^2)	3.2045(fix)	3.2045(fix)	3.2045(570)	3.2072(1130)	3.2072(fix)	3.2072(fix)
F (GHz)	169.39	169.47	169.50	167.91	167.93	167.96
λ_a	0.80686(518)	0.80778(437)	0.80562(431)	0.81486(534)	0.81352(550)	0.81218(658)
λ_b	0.59074	0.58949	0.59244	0.57966	0.58154	0.58340
λ_c	0.0	0.0	0.0	0.0	0.0	0.0
V_3(cal/mol)	936.1 (6)	935.9 (5)	937.2 (4)	931.2 (7)	932.9 (8)	934.9 (10)
θ[b]	36°13'(30')	36°07'(26')	36°20'(25')	35°26'(32')	35°34'(33')	35°41'(39')
RMS (MHz)	0.10	0.08	0.08	0.07	0.08	0.09
max.dev.[c] (MHz)	0.20	0.24	0.26	0.28	0.20	0.27
θ_{st}[d]	34°15'	34°14'	34°14'	33°42'	33°42'	33°41'
$\Delta\theta$[e]	1°50'	1°53'	2° 6'	1°44'	1°52'	2°
I_α (3.1276 amu·Å^2) and direction cosines were fixed at the values calculated from the r_s structure.						
V_3(cal/mol)	958.9 (44)	947.7 (70)	947.2 (72)	946.3 (51)	948.2 (56)	950.7 (61)
RMS (MHz)	0.73	0.56	0.61	0.50	0.55	0.59
max.dev. (MHz)	1.63	1.47	1.50	1.26	1.67	1.70

		$^{13}CH_3GeH_2F$			CD_3GeH_2F	
	^{74}Ge	^{72}Ge	^{70}Ge	^{74}Ge	^{72}Ge	^{70}Ge
A (MHz)	13170.819(116)	13250.442(111)	13333.640(129)	11797.252(65)	11866.545(70)	11939.050(79)
B (MHz)	6059.445(35)	6059.454(33)	6059.430(38)	5375.929(32)	5376.537(32)	5377.098(33)
C (MHz)	4496.910(34)	4506.215(33)	4515.846(38)	4067.128(31)	4075.696(31)	4084.587(31)
Δ_J (kHz)	6.63(209)	8.24(199)	6.96(231)	6.10(189)	6.33(188)	4.06(193)
Δ_{JK} (kHz)	-35.80(242)	-38.24(231)	-36.57(282)	-26.51(118)	-23.08(123)	-25.17(124)
Δ_K (kHz)	163.70(2434)	193.74(2316)	160.13(2704)	89.97(1384)	105.83(1481)	107.43(1688)
δ_J (kHz)	2.51(12)	2.28(11)	2.28(13)	1.44(6)	1.66(6)	1.45(6)
δ_K (kHz)	-0.27(154)	1.00(150)	1.20(178)	2.98(112)	-0.47(131)	3.50(130)
I_α (amu.Å)	3.2068(fix)	3.2068(fix)	3.2068(1795)	6.4041(fix)	6.4041(fix)	6.4041(fix)
F (GHz)	169.31	169.36	169.43	90.43	90.50	90.51
λ_a	0.82574(1171)	0.82453(867)	0.82462(925)	0.85323(4839)	0.85317(4578)	0.84954(4866)
λ_b	0.56405	0.56582	0.56570	0.52154	0.52163	0.52752
λ_c	0.0	0.0	0.0	0.0	0.0	0.0
V_3(cal/mol)	933.4 (11)	934.7 (12)	935.2 (13)	904.8 (45)	907.1 (46)	909.2 (51)
θ[b]	34°20'(1°11')	34°28'(53')	34°27'(56')	31°26'(5°19')	31°26'(5°02')	31°50'(5°17')
RMS (MHz)	0.08	0.08	0.09	0.06	0.06	0.06
max.dev.(MHz)	0.16	0.20	0.20	0.16	0.17	0.20
θ_{st}[d]	32°43'	32°44'	32°44'	28°58'	29° 1'	29° 5'
$\Delta\theta$	1°37'	1°44'	1°43'	2°28'	2°25'	2°45'
I_α (3.1276 amu·Å) and direction cosines were fixed at the values calculated from the r_s structure.						
V_3(cal/mol)	951.8 (42)	950.9 (44)	951.7 (44)	928.1 (63)	930.6 (65)	933.1 (71)
RMS (MHz)	0.30	0.28	0.28	0.08	0.08	0.09
max.dev.(MHz)	0.78	0.58	0.56	0.22	0.21	0.26

---

[a] The Watson-A reduction formula was used.
[b] The angle between the methyl top axis and the a-inertial axis, obtained from the direction cosine, λ_a.
[c] The absolute maximum deviation between the observed and calculated frequencies.
[d] The angle between the methyl top axis and the a-inertial axis calculated from the r_s coordinate values
[e] $\Delta\theta=\theta-\theta_{st}$.

rotational constants between the + and − states were actually very small; that is, for the *a*-$CH_2D^{74}GeH_2F$ species, $(\Delta A, \Delta B, \Delta C) = (1.53, 0.12, -0.15)$ MHz, where $\Delta G = G^+ - G^-$ ($G = A, B$, and C).

The energy levels of the + and − states were calculated from the rotational constants and the centrifugal distortion constants obtained above and the energy difference between the + and − states, $\Delta E^0(-, +)$.

TABLE IVb

Rotational and Centrifugal Distortion Constants[a] of CH_2DGeH_2F Species

		^{74}Ge	^{72}Ge	^{70}Ge
			s-CH_2DGeH_2F	
A	(MHz)	13339.847(20)	13418.727(23)	13501.386(17)
B	(MHz)	5810.308(8)	5810.270(9)	5810.327(7)
C	(MHz)	4378.620(8)	4387.091(9)	4395.994(7)
Δ_J	(kHz)	6.28 (50)	3.84 (58)	6.28 (44)
Δ_{JK}	(kHz)	-31.83 (36)	-29.60 (40)	-30.02 (28)
Δ_K	(kHz)	144.37 (441)	139.09 (492)	117.34 (372)
δ_J	(kHz)	1.92 (2)	1.94 (2)	1.89 (1)
δ_K	(kHz)	2.33 (38)	1.85 (37)	2.10 (27)
RMS	(MHz)	0.02	0.02	0.02
N^b		27	28	29
			a-CH_2DGeH_2F +State	
A	(MHz)	12516.124(91)	12589.988(109)	12667.751(112)
B	(MHz)	5995.030(28)	5995.046(36)	5995.165(42)
C	(MHz)	4437.798(27)	4447.082(35)	4456.874(39)
Δ_J	(kHz)	5.76 (179)	2.28 (230)	5.46 (258)
Δ_{JK}	(kHz)	-36.76 (160)	-36.60 (212)	-37.12 (238)
Δ_K	(kHz)	144.19 (1967)	123.73 (2212)	153.47 (2461)
δ_J	(kHz)	2.54 (7)	2.62 (11)	2.62 (11)
δ_K	(kHz)	0.93 (156)	1.20 (225)	0.68 (268)
			a-CH_2DGeH_2F -State	
A	(MHz)	12514.620(73)	12588.544(127)	12666.080(129)
B	(MHz)	5994.905(28)	5994.891(35)	5995.007(43)
C	(MHz)	4437.964(27)	4447.246(35)	4457.010(39)
Δ_J	(kHz)	13.99 (186)	10.13 (226)	13.14 (283)
Δ_{JK}	(kHz)	-36.29 (164)	-36.82 (216)	-35.62 (242)
Δ_K	(kHz)	152.37 (1658)	138.19 (2508)	106.39 (2790)
δ_J	(kHz)	2.58 (7)	2.47 (11)	2.60 (11)
δ_K	(kHz)	-1.17 (155)	1.13 (225)	0.93 (270)
Q	(MHz)	8.07 (178)	10.77 (158)	9.44 (216)
ΔE	(MHz)	180.0 (ass)	180.0 (ass)	180.0 (ass)
RMS	(MHz)	0.05	0.06	0.07
N^b		46	43	43
A_{ave}^c	(MHz)	12515.372(82)	12589.266(118)	12666.915(120)
B_{ave}	(MHz)	5994.968(28)	5994.968(36)	5995.086(42)
C_{ave}	(MHz)	4437.881(27)	4447.164(35)	4456.942(39)
ΔA^d	(MHz)	1.504	1.444	1.671
ΔB	(MHz)	0.125	0.155	0.158
ΔC	(MHz)	-0.166	-0.164	-0.136

a. The Watson-A reduction formula was used.
b. Number of frequencies used.
c. Gave = $(G^+ + G^-)/2$.
d. $\Delta G = G^+ - G^-$.

It was found that there is no possibility of near degeneracy within 50 MHz for the energy levels with $J \leqslant 8$ in the interval of the $\Delta E^0(-, +)$ value between 150 and 250 MHz.

From the above facts, the splittings of the spectra for the *a*-CH_2DGeH_2F species are considered to arise mainly from the small differences of the rotational constants of the + and − states which are composed from many perturbation terms with small magnitudes.

The connecting terms between the + and − states are also composed from many perturbation terms with small magnitudes.

Hence, we cannot calculate the rotational constants containing the internal rotation contributions and the coefficients of the connecting terms to sufficient accuracy in a manner similar to the symmetric internal rotor such as the CH_3 group.

Therefore, we gave up the attempt to determine the V_3 value from the splittings between the + and − states and tried to obtain the coefficients *Q*, *N*, *E*, and *D* in the following Hamiltonian given by Quade *et al.*, experimentally as merely the adjustable parameters:

$$\langle + | H | + \rangle = A^+P_a^2 + B^+P_b^2 + C^+P_c^2 + H^+_{\text{cent}}$$

$$\langle - | H | - \rangle = A^-P_a^2 + B^-P_b^2 + C^-P_c^2 + H^-_{\text{cent}} + \Delta E$$

$$\langle + | H | - \rangle = QP_a + NP_b + E(P_aP_c + P_cP_a) + D(P_bP_c + P_cP_b).$$

For the centrifugal distortion terms, H^+_{cent} and H^-_{cent}, the Watson-A reduction formula was used.

Assuming ΔE = 180.0 MHz, an attempt was made to determine four coefficients Q, E, N, and D of the terms in the connecting matrix elements by a least-squares calculation. It was found that Q and D terms in the Hamiltonian produce some improvements for the fit of the observed frequencies, while E and N terms do not. Furthermore, as Q and D terms show a similar behavior with each other for the fit of the present observed frequencies, the use of one of Q and D terms is sufficient to predict the frequencies.

Hence, we decided to use the Q term for the fit since the error limit of the coefficient of the Q term was obtained to be much smaller than that of the D term. As already mentioned, the ΔE is insensitive for the present observed frequencies. The quantities determined are listed in Table IVb and the differences between the observed and calculated frequencies are given in Table IIIc.

The average of the rotational constants for the + and − states listed in Table IVb was used for the determination of the r_s structure.

r_s STRUCTURE

The present data are sufficient to determine the r_s coordinates of all the atoms in the molecule except those of the fluorine atom which have to be solved with the aid of the first moment equations.

The r_s coordinates were computed by the Kraitchman equations from the moments of inertia determined from the observed rotational constants. The coordinates of the atoms in the molecular plane were solved by Chutjian type Kraitchman equations according to the remarks given by Rudolph (*8*).

The coordinates of the atoms which could be solved from several sets of the parent and isotopic species were taken to be the average values of these sets after the appropriate transformation between the principal axes systems was carried out when the parent species of a given set was not the normal species. The procedures of these calculations were already described in our previous paper (*3*).

There are three atom coordinates whose values are so small that the solutions of the Kraitchman equations cannot be reliable. They are x_a(Ge), x_a(H) of the GeH$_2$ group, the x_b(H$_s$) of the CH$_3$ group. Since the coordinates of the fluorine atom are solved by the first moment equations, these unreliable coordinates should be fixed by the other relations. For the x_b coordinate of the H$_s$ hydrogen atom in the CH$_3$ group, the Kraitchman value gives 1.047 Å for the r(CH$_s$) bond length which is too small to be accepted and a structural assumption of $r(\text{CH}_s) = r(\text{CH}_a)$ was used to fix the value. The x_a of the germanium atom was fixed by the zero inertia product condition,

$I_{ab} = 0$, while the x_a of the hydrogen atom in the GeH_2 group was assumed at first to be the Kraitchman value although its magnitude was small. Several trials were made to fix the x_a of the hydrogen atom.

However, reasonable results could not be obtained. Then, we decided to use the Kraitchman value in spite of its smallness. The adequacy of the present choice for the x_a coordinate of the hydrogen atom in the GeH_2 group will be proved passively when we compare the structural parameters of the GeH_2 group with the corresponding parameters of the analogous molecules.

The differences between the observed and calculated moments of inertia are included in Table V, and the r_s coordinates thus obtained are listed in Table VI. The differences are small and positive for all the species and the RMS value is 0.20145 amu • Å^2 so that the r_s structure is considered to be well established.

DISCUSSIONS

Structure

In Table VII, the structural parameters calculated from the r_s coordinates are listed where the parameters for the analogous molecules, ethyl fluoride and methyl fluorosilane, are also listed.

For ethyl fluoride and methyl fluorosilane, the parameters in the previous papers (*3, 9, 11*) were calculated from the r_s coordinates obtained by different choices of the assumptions to the case of the present molecule. Hence, we recalculated them with the same assumptions.

TABLE V

Moments of Inertia of Methyl Fluorogermane (amu • Å^2)^a

Species	I_a	δI_a^{b}	I_b	δI_b^{b}	I_c	δI_c^{b}	P_c^{c}	ΔP_c^{c}
$CH_3{}^{74}GeH_2F$	37.82765(29)	0.01846	80.83772(50)	0.10342	109.26985(90)	0.32283	4.69776(84)	
$CH_3{}^{72}GeH_2F$	37.60655(24)	0.01970	80.83822(43)	0.10413	109.04850(75)	0.32402	4.69814(71)	0.00038(155)
$CH_3{}^{70}GeH_2F$	37.37722(23)	0.02095	80.83824(40)	0.10436	108.81766(70)	0.32397	4.69890(67)	0.00114(151)
$CH_3{}^{74}GeD_2F$	43.70283(27)	0.01861	84.11782(41)	0.10349	111.98510(70)	0.32285	7.91777(69)	3.22001(153)
$CH_3{}^{72}GeD_2F$	43.50917(29)	0.02020	84.11799(43)	0.10387	111.79057(74)	0.32377	7.91829(73)	3.22054(157)
$CH_3{}^{70}GeD_2F$	43.30764(34)	0.02101	84.11845(52)	0.10454	111.58913(89)	0.32488	7.91848(87)	3.22072(172)
$^{13}CH_3{}^{74}GeH_2F$	38.37089(34)	0.01758	83.40302(48)	0.09890	112.38295(85)	0.32198	4.69548(84)	-0.00228(168)
$^{13}CH_3{}^{72}GeH_2F$	38.14031(32)	0.01834	83.40289(45)	0.09914	112.15089(82)	0.32162	4.69616(80)	-0.00160(164)
$^{13}CH_3{}^{70}GeH_2F$	37.90233(37)	0.02018	83.40322(52)	0.09985	111.91170(94)	0.32264	4.69693(92)	-0.00083(176)
$CD_3{}^{74}GeH_2F$	42.83845(24)	0.08180	94.00719(56)	0.10619	124.25869(95)	0.33938	6.29348(87)	1.59572(172)
$CD_3{}^{72}GeH_2F$	42.58830(25)	0.08246	93.99656(56)	0.10652	123.99747(94)	0.33992	6.29370(88)	1.59594(172)
$CD_3{}^{70}GeH_2F$	42.32967(28)	0.08377	93.98676(58)	0.10796	123.7256 (94)	0.34121	6.29443(90)	1.59667(174)
s-$CH_2D^{74}GeH_2F$	37.88469(6)	0.06084	86.97921(12)	0.12789	115.41901(21)	0.34030	4.72245(19)	0.02469(104)
s-$CH_2D^{72}GeH_2F$	37.66199(7)	0.06191	86.97978(14)	0.12889	115.19615(24)	0.34164	4.72281(22)	0.02505(106)
s-$CH_2D^{70}GeH_2F$	37.43142(5)	0.06331	86.97893(11)	0.12848	114.96285(18)	0.34076	4.72375(17)	0.02599(101)
a-$CH_2D^{74}GeH_2F$	40.38042(27)	0.02047	84.30003(39)	0.09999	113.87777(69)	0.32064	5.40134(68)	0.70358(152)
a-$CH_2D^{72}GeH_2F$	40.14341(38)	0.02214	84.30003(51)	0.10109	113.64006(89)	0.32257	5.40169(89)	0.70393(173)
a-$CH_2D^{70}GeH_2F$	39.89732(38)	0.02351	84.29837(59)	0.10056	113.39075(99)	0.32170	5.40247(98)	0.70471(182)

a. Figures in parentheses indicate the uncertainties attached to the last digit.
b. The differences between the observed and calculated moments of inertia. The calculated I_g was computed from the r_s coordinate values listed in Table VI.
c. $P_c=(I_a+I_b-I_c)/2$. $\Delta P_c=P_c(\text{isotopic})-P_c(\text{normal})$.

TABLE VI

Atom Coordinates (Å)[a]

	x_a	x_b	x_c
F[b]	1.33339(1044)	0.77376(581)	0
Ge	-0.01004(252)[c]	-0.33045(121)	0
H	0.16893(211)	-1.15987(35)	±1.26488(3)
C	-1.59745(52)	0.76159(113)	0
H_a	-1.62018(52)	1.38670(66)	±0.88350(103)
H_s	-2.47637(22)	0.12964(542)[d]	0

a. Root-mean square deviation between the observed and calculated moments of inertia for eighteen isotopic species is 0.20145 amu·$Å^2$.

b. Coordinate values were solved by the first moment equations.

c. Solved by $I_{ab}=0$ condition.

d. Solved under the assumption of $r(CH_s)=r(CH_a)$.

"M" indicates C, Si, and Ge atoms hereafter in this section. For the skeleton, $r(MF)$ values are larger than those for MH_3F molecules (*12, 13, 14*) and the ratios of elongation are 0.36, 0.57, and 0.40% for M = C, Si, and Ge, respectively. On the other hand, $r(CM)$ values are smaller than those for CH_3MH_3 molecules (*15, 16, 17*) and the ratio of shortening decreases from C to Ge (1.32, 1.17, 0.94%). The angle α(CGeF) (106°3′) is much smaller than the corresponding angles for methyl fluorosilane and ethyl fluoride (109°15′, 109°34′).

For the MH_2 group, $r(MH)$ values are smaller than those of CH_3MH_3 molecules and the ratio of shortening decreases from C to Ge (0.70, 0.47, 0.39%).

As for the angles around the M atom, very interesting results are noted; that is, the angle $\alpha(MHF)$ is much smaller than the angle $\alpha(HMC)$ for all the CH_3MH_2F type molecules. This fact is also found for ethyl halides, methyl chlorogermane, and methyl bromogermane (*9, 18, 19, 11, 20, 21*).

As shown in Fig. 1, we can define δ as the angle between the bisector plane of the $\alpha(CMF)$ angle and the MH_2 plane. δ can be computed as follows:

$$\delta = (\beta(HMC) - \beta(HMF))/2$$

$$\cos(\beta(HMC)) = \cos(\alpha(HMC))/\cos(\alpha(HMH)/2)$$

$$\cos(\beta(HMF)) = \cos(\alpha(HMF))/\cos(\alpha(HMH)/2).$$

For ethyl halides, the values for δ are 5°23′, 5°, 6°55′, and 7°44′ for fluoride, chloride, bromide, and iodide, respectively. For CH_3MH_2F molecules, they are 5°23′, 6°18′, and 9°30′ for M = C, Si, and Ge, respectively, and for CH_3GeH_2X molecules, they are 9°30′, 6°46′, and 5°29′ for X = F, Cl, and Br, respectively.

This relation is also found for CH_3X molecules (*12*), that is, when one of the three hydrogen atoms is considered to be the group corresponding to the CH_3 group of CH_3MH_2X molecules, the values of δ are 2°, 2°38′, 3°31′, and 3°36′, for X = F, Cl, Br, and I, respectively.

For all the molecules, it is important to note that the δ values are always positive so that the two hydrogen atoms of the MH_2 group incline to the halogen atom and

TABLE VII

Structural Parameters[a] of Analogous Molecules

	CH_3GeH_2F		CH_3SiH_2F		CH_3CH_2F
	This work	Robert et al(ref.1)	Recalculated[b]	Reported(Ref.3)	ref.9
Skeleton					
r(MF) (Å)	1.739(14)	1.752	1.602(9)	1.597(9)	1.387(3)
r(CM) (Å)	1.927(4)	1.925	1.845(4)	1.847(5)	1.512(2)
α(CMF)	106° 3'(53')	106°18'	109°15'(47')	109° 9'(39')	109°34'(21')
MH_2					
r(MH) (Å)	1.523(2)	1.525(ass)	1.478(2)	1.478(2)	1.094(1)
α(HMC)	113°55'(17')	108°55'(ass)	112°27'(18')	112°17'(16')	112°14'(8')
α(HMF)	104°46'(24')	111°17'(ass)	106°12'(21')	106°26'(28')	106°49'(8')
α(HMH)	112°17'(15')	110° (ass)	109°51'(16')	109°53'(5')	108°53'(5')
δ^c	9°30'(22')	-2° (ass)	6°18'(43')	5°54'(57')	5°23'(19')
CH_3					
$r(CH_s)$	1.083(ass)	1.093(ass)	1.089(ass)	1.105(5)	1.093(ass)
$r(CH_a)$	1.083(2)	1.093(ass)	1.089(1)	1.089(1)	1.093(1)
$\alpha(MCH_s)$	109°45'(52')	109°50'	109°39'(46')	108°43'(39')	109°43'(20')
$\alpha(MCH_a)$	110° 9'(19')	109°50'	111°22'(17')	111°20'(26')	110°16'(6')
$\alpha(H_sCH_a)$	108°39'(23')	109° 6'	107°50'(17')	108°23'(28')	108°50'(6')
$\alpha(H_aCH_a)$	109°24'(25')	109° 6'	108°39'(13')	108°34'(4')	108°51'(4')
γ^d	110° 1'(30')	109°50'	110°48'(27')	110°28'(30')	110° 5'(17')
θ^e	16'(47')	0 (ass)	1° 9'(42')	1°45'(43')	22'(17')
β^f	-45'(48')	0 (ass)	-49'(30')	-11'(32')	-1'(10')
$I_\alpha(st)^i$ (amu·Å^2)	3.1276		3.1789		3.1843
$\theta_{int}{}^g$	-1°58'(30')	-1°54'	-47'	-47'	-32'(25')[h]
$I_\alpha(int)^j$	3.2045(570)		——		3.155 (14)[h]
$\Delta\theta=\theta-\theta_{int}$	2°14'	1°54'	1°56'	2°32'	

a. Figures in parentheses indicate uncertainties attached to the last digit calculated from 2.5 times the standard deviation.

b. For methyl fluorosilane, the parameter values were obtained by different choices of the condition in the previous paper. Then, they were re-calculated by the same conditions as the case of methyl fluorogermane.

c. The angle between the MH_2 plane and the bisector plane of the angle α(FMC). See the t

d. The unperturbed MCH angle.

e. The tilt angle obtained from the structure.

f. The difference between $\alpha(H_sCH_a)$ and $\alpha(H_aCH_a)$.

g. The tilt angle obtained from the A-E splitting analysis.

h. Calculated from the data in Ref. 10.

i. The methyl top moment of inertia calculated from the r_s structure.

j. The methyl top moment of inertia obtained from the A-E splitting analysis.

the δ increases in the order of C, Si, and Ge. It is very difficult to interpret this tendency at present. If this relation comes from the steric repulsion between the hydrogen and halogen atoms, δ should decrease from C to Ge. We are working at present to determine whether or not this fact can be predicted by MO calculations.

One of the differences of the r_s structures between this work and that reported by Roberts *et al.* (*1*) is the difference of the angle relation mentioned above. Roberts *et al.* transferred the angle of CH_3GeH_3 and GeH_3F molecules to those of the present molecule and their α(HGeC) is smaller than the α(HGeF).

For the CH_3 group, the x_b coordinate of the H_s hydrogen atom for all the CH_3MH_2F molecules is so small that it is fixed by the $r(CH_s) = r(CH_a)$ assumption. For $r(CH_a)$, the value decreases from C to Ge. For CH_3MH_3 molecules, r(CH) also decreases from C to Ge (1.102, 1.093, 1.083 Å).

For the examination of the angle relations of the methyl group, the following three angles are defined as in the previous paper (*3*). The unperturbed MCH angle γ defined by

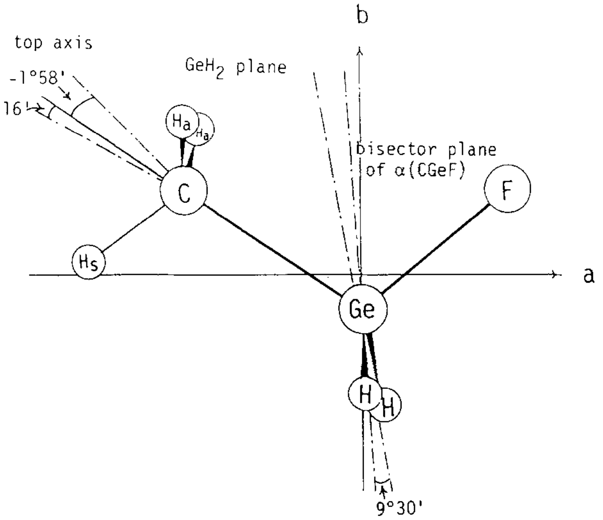

FIG. 1. The bisector plane of α(CGeF), the GeH$_2$ plane, and the top axis of the methyl group of methyl fluorogermane.

$$\gamma = \tfrac{1}{3}[2\alpha(M\mathrm{CH_a}) + \alpha(M\mathrm{CH_s})]$$

which indicates whether or not the methyl group is slender. The tilt angle θ defined by

$$\theta = \tfrac{2}{3}[\alpha(M\mathrm{CH_a}) - \alpha(M\mathrm{CH_s})]$$

which corresponds to the angle between the methyl internal top axis and the MC bond when the three CH bond lengths are equal to each other since the internal top axis is defined by the direction of the normal line of the plane made by the three hydrogen atoms in the methyl group and the axis passes through the center of masses of the three hydrogen atoms.

The angle β defined by

$$\beta = \alpha(\mathrm{H_sCH_a}) - \alpha(\mathrm{H_aCH_a})$$

indicates whether or not the methyl group is flat along the molecular plane.

For CH_3MH_2F molecules, γ is larger than the tetrahedral angle and the methyl top is slender. θ is very small for ethyl fluoride and methyl fluorogermane while it is 1°9′ for methyl fluorosilane. It is noted that θ is positive for CH_3MH_2F molecules and the methyl group tilts toward the two hydrogen atoms of the MH_2 group.

For ethyl fluoride, β is small, while they are −49′ and −45′ for methyl fluorosilane and germane, respectively.

In Table VII, the tilt angle obtained from the A–E splitting analysis is also listed as θ_{int}.

It is noted that θ_{int} values are negative for all the CH_3MH_2F molecules so that the methyl group is considered to be tilted toward the fluorine atom from the A–E splitting analysis.

The difference $\Delta\theta$ between θ and θ_{int} is more than 1° and is significant even though the error limit is large.

Roberts *et al.* assumed the tilt angle obtained from the A–E splitting analysis when their r_s structure was established and they concluded that the methyl group tilted toward the fluorine atom.

However, as already mentioned in the previous papers (*3, 5*), the methyl tilt angle obtained from the A–E splitting analysis has not always coincided with that from the r_s structure. When θ is not zero, θ_{int} is always smaller than θ so that θ_{int} is negative for methyl fluorogermane.

Methyl Internal Rotation

From the r_s coordinates, the methyl top moment of inertia, I_α around the top axis could be calculated to be 3.1276 amu · Å^2 which is smaller than the value (3.2045 amu · Å^2) determined from the A–E splitting analysis mentioned in the earlier section. For methyl fluorosilane, we used the I_α calculated from the r_s structure. For ethyl fluoride, Dreizler *et al.* (*10*) could determine the I_α from the A–E splitting analysis and the value is 3.155 amu · Å^2 which is smaller than the I_α calculated from the r_s coordinates (3.1843 amu · Å^2).

In the previous paper (*5*), we reported that the I_α values obtained from the A–E splitting analysis (3.1889 and 3.2084 amu · Å^2) are larger than the ones calculated from the r_s coordinates for dimethyl silane and dimethyl sulfide, viz., 3.1234 and 3.1953 amu · Å^2.

For methyl fluorogermane, the difference between the two I_α values corresponds to elongation of the distance of a hydrogen atom from the top axis by about 0.16 Å. A similar result was already reported by Bauder and Gunthard (*22*) for acetaldehyde and they suggested that it is due to the vibrational interactions and the structural relaxations.

The calculations of the A–E splitting fit were carried out assuming the I_α and direction cosines of the top axis calculated from the r_s coordinates and regarding V_3 as a variable. The results are listed briefly in Table IVa. The RMS and absolute maximum deviations of the fit become fairly worse and the error limits of the V_3 values increase. The same tendencies have already been found for dimethyl silane and sulfide in the previous paper (*5*).

The choice of I_α affects the V_3 value. When the I_α is assumed to be the value from the A–E splitting analysis, the V_3 is 935 ± 3 cal/mol which is the average of nine species having the CH_3 group, while the V_3 is 907 ± 3 cal/mol for the species with the CD_3 group. The V_3 of the CD_3 group is smaller by about 3% than that of the CH_3 group. For acetone, Nelson and Pierce (*23*) found a similar result. The V_3 for $(CD_3)_2CO$ is smaller by about 6.5% as compared with the V_3 of $(CH_3)_2CO$.

RECEIVED: January 3, 1989

REFERENCES

1. R. F. ROBERTS, R. VARMA, AND J. F. NELSON, *J. Chem. Phys.* **64**, 5035–5050 (1976).

2. L. C. KRISHER AND J. A. MORRISON, *J. Chem. Phys.* **64**, 3556–3559 (1976).

3. Y. SHIKI, M. OYAMADA, AND M. HAYASHI, *J. Mol. Spectrosc.* **92**, 375–390 (1982).

4. C. R. QUADE AND C. C. LIN, *J. Chem. Phys.* **38,** 540–550 (1963).

5. M. HAYASHI, N. NAKATA, AND S. MIYAZAKI, *J. Mol. Spectrosc.*, **135,** 270–288 (1989).

6. J. K. G. WATSON, *in* "Vibrational Spectra and Structure, A Series of Advances," Vol. 6, pp. 1–89, Elsevier, New York, 1977.

7. P. H. TURNER, A. P. COX, AND J. A. HARDY, *J. Chem. Soc. Faraday Trans. 2* **77,** 1217–1231 (1981).

8. H. D. RUDOLPH, *J. Mol. Spectrosc.* **89,** 460–464 (1981).

9. M. HAYASHI, M. FUJITAKE, T. INAGUSA, AND S. MIYAZAKI, *J. Mol. Struct.*, in press.

10. E. FLIEGE, H. DREIZLER, J. DEMAISON, D. BONCHER, J. BURIE, AND A. DUBRULLE, *J. Chem. Phys.* **78,** 3541–3544 (1983).

11. T. INAGUSA, M. FUJITAKE, AND M. HAYASHI, *J. Mol. Spectrosc.* **128,** 456–468 (1988).

12. J. L. DUNCAN, *J. Mol. Struct.* **6,** 447–456 (1970).

13. A. G. ROBIETTE, G. J. CARTWRIGHT, A. R. HOY, AND I. M. MILLS, *Mol. Phys.* **20,** 541–553 (1971).

14. L. C. KRISHER, J. A. MORRISON, AND W. A. WATSON, *J. Chem. Phys.* **57,** 1357–1358 (1972).

15. K. KUCHITSU, *J. Chem. Phys.* **49,** 4456–4462 (1968).

16. R. W. KILB AND L. PIERCE, *J. Chem. Phys.* **27,** 108–112 (1957).

17. V. W. LAURIE, *J. Chem. Phys.* **30,** 1210–1214 (1959).

18. T. INAGUSA AND M. HAYASHI, to appear.

19. T. INAGUSA AND M. HAYASHI, *J. Mol. Spectrosc.* **129,** 160–171 (1988).

20. W. ZEIL AND D. CHRISTEN, *J. Phys. Chem.* **84,** 1790–1792 (1980).

21. J. R. DURIG, J. F. SULLIVAN, A. B. MOHAMAD, S. CRADOCK, AND Y. S. LI, *J. Chem. Phys.* **84,** 5796–5809 (1986).

22. A. BAUDER AND HS. H. GÜNTHARD, *J. Mol. Spectrosc.* **60,** 290–311 (1976).

23. R. NELSON AND L. PIERCE, *J. Mol. Spectrosc.* **18,** 344–352 (1965).